Available online at www.sciencedirect.com
SCIENCE DIRECT
Remote Sensing of Environment 95 (2005) 453–463
Remote Sensing of Environment
www.elsevier.com/locate/rse

Evaluation of spring snow covered area depletion in the Canadian Arctic from NOAA snow charts

Libo Wang[a,*], Martin Sharp[a], Ross Brown[b], Chris Derksen[c], Benoit Rivard[a]

[a]Earth and Atmospheric Sciences, University of Alberta, Edmonton, AB, Canada T6G 2E3
[b]Climate Research Branch, Meteorological Service of Canada, Dorval, QC, Canada
[c]Climate Research Branch, Meteorological Service of Canada, Downsview, ON, Canada

Received 22 September 2004; received in revised form 26 January 2005; accepted 29 January 2005

Abstract

The National Oceanic and Atmospheric Administration (NOAA) weekly snow cover dataset (1966–) is the longest available record of snow cover extent (SCE) over the Northern Hemisphere (NH). This dataset has been used extensively to derive trends in continental SCE and in climate-related studies, but it has received only limited validation, particularly in high latitude areas of the NH. This study evaluated spring snow cover depletion in the NOAA dataset over a study area in the Canadian Arctic mainland north of the tree line. The evaluation used four sources of information: (1) surface snow depth and snow survey observations, (2) snow cover extent produced from the Advanced Very High Resolution Radiometer (AVHRR), (3) snow cover extent derived from Special Sensor Microwave/Imager (SSM/I), and (4) Landsat 5 TM browse images. Six spring seasons from the period 1981–2000 with low (1984, 1988, and 1998) and high (1985, 1995, and 1997) spring snow cover extent were evaluated. The evaluation revealed that the NOAA weekly dataset consistently overestimated snow cover extent during the spring melt period, with delays of up to 4 weeks in melt onset. A number of possible reasons for this delay were investigated. The most likely causes for the delayed melt onset were frequent cloud cover in the spring melt period, and the low frequency of data coverage over higher latitudes. The results suggest that caution should be exercised when using this dataset in any studies related to the timing of snowmelt in the high latitudes of the Northern Hemisphere.

Keywords: NOAA snow charts; Snow cover extent; Spring melt; Canadian arctic

1. Introduction

Snow cover extent (SCE) over the Northern Hemisphere (NH) landmass has been continuously monitored by the National Oceanic and Atmospheric Administration (NOAA) since 1966 (Dewey & Heim, 1981). The NOAA weekly snow cover product is the longest time series of spatially continuous snow cover data available for the NH. It consists of digitized weekly charts of snow cover derived from the visual interpretation of visible satellite imagery by trained analysts. This dataset has been widely used to document regional and hemispheric variability in snow cover extent (Brown, 2000; Dye, 2002; Easterling et al., 2000; Frei & Robinson, 1999; Iwasaki, 1991; Robinson et al., 1993). Trends in continental SCE from the NOAA dataset were presented in the latest Intergovernmental Panel on Climate Change (IPCC) assessment report (IPCC, 2001, p124). A global decrease in spring SCE derived from the NOAA dataset partially explains the significant increase in spring surface air temperature over the NH landmass during the past century (Groisman et al., 1994a). In addition, Saunders et al. (2003) used the NOAA dataset to demonstrate a statistically significant linkage between summer NH SCE and the North Atlantic Oscillation pattern in the following winter.

Brown and Alt (2001), however, found major discrepancies between SCE estimates derived from in situ snow depth observations and those from the NOAA dataset over the Canadian Arctic (the area contributing much of the summer season variability in NH SCE). To date, the

* Corresponding author. Tel.: +1 780 4924783; fax: +1 780 4927598.
E-mail address: libo@ualberta.ca (L. Wang).

0034-4257/$ - see front matter © 2005 Elsevier Inc. All rights reserved.
doi:10.1016/j.rse.2005.01.006

NOAA dataset has received only limited validation (Kukla & Robinson, 1981; Robinson & Kukla, 1988; Wiesnet et al., 1987), especially in the NH high latitudes. Kukla and Robinson (1981) performed the most detailed evaluation of the NOAA snow charts. They reproduced an independent set of snow maps for selected blocks of the United States and Asia by re-charting satellite imagery with the assistance of ground observations. Snow coverage, in percent of total area derived from the NOAA weekly charts, was compared to daily snow coverage for selected weeks in November, January, February, and March. The average differences were found to be less than 10% of the area of the block. The best match was obtained for the last or the penultimate day of the week. However, large discrepancies were often found in the NOAA charts for autumn, especially for Asia. Robinson et al. (1993) concluded that the accuracy of the winter and spring charts was sufficient for continental or hemispheric scale climate-related studies. Nevertheless, the NOAA dataset has never been evaluated for the Arctic regions, which are widely believed to be especially sensitive to anthropogenic climate change. This is mainly because ground observations in these regions are sparse, making validation of the NOAA dataset more difficult.

The NOAA dataset has frequently been compared to other snow cover products. These include passive microwave derived snow products (Special Sensor Microwave/Imager-SSM/I, operational 1987 to present; Scanning Multichannel Microwave Radiometer-SMMR, operational 1978–1987), the U.S. Air Force daily global snow cover dataset, and the National Operational Hydrological Remote Sensing Center snow cover dataset (Armstrong & Brodzik, 2001; Basist et al., 1996; Pivot et al., 2002; Scialdone & Robock, 1987). In most cases, however, the NOAA dataset has been taken more or less as the standard during these comparisons. In this paper, the NOAA dataset was evaluated for the region of the Canadian Arctic mainland north of the tree line (Fig. 1) during the spring melt period. This particular study area was selected to minimize forest-masking effects, and to avoid problems related to the coarse resolution of the NOAA product over the Canadian Arctic Archipelago. The evaluation focused on six spring periods from the 1981–2000 period with unusually low (1984, 1988, and 1998) or high (1985, 1995, and 1997) SCE over North America. The spring period was selected because the snow line migration can be tracked for several weeks through the study region, unlike the fall season when the entire region becomes completely snow covered in a very short period. There was also an interest in looking at the spring melt period from a snow cover-climate feedback perspective since this is the period when snow cover exhibits the strongest feedback to the climate system (Groisman et al., 1994b). The NOAA dataset was compared to snow cover extents derived from AVHRR, SSM/I, and Landsat 5 TM browse images, and surface snow observations. A number of variables including cloud cover, lake ice, and fractional snow cover thresholds were explored in an attempt to explain differences between the various datasets.

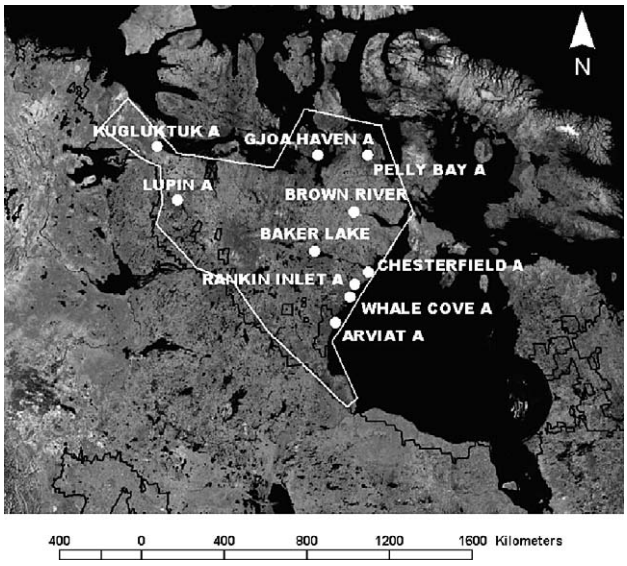

Fig. 1. Study area (white outline) overlaid on 1000 m resolution Radarsat mosaic downloaded from http://geogratis.cgdi.gc.ca. White dots are snow depth observation stations and black contour stands for forest cover >0 derived from IGBP land cover classification.

2. Study area

The study area is located on the northwest side of Hudson Bay (Fig. 1), between latitudes 58° N~70° N, and longitudes 85° W~122° W. This area is located above the tree line and is dominated by barren tundra according to the IGBP land cover classification (Loveland et al., 2000). The study area is relatively flat, with elevations generally below 500 m. This area experiences the longest period of seasonal snow cover on the North American mainland and contributes a large fraction of the NH SCE in spring/summer. Ten snow depth observation stations are located in the study area (Fig. 1), although the number that were operational varied from year to year. There are also a few snow survey observations in the study area, but none are available during May or June when the NOAA dataset exhibits the largest difference from the other datasets.

3. Data and methods

3.1. NOAA weekly snow cover dataset

From November 1966 to May 1999 the National Oceanic and Atmospheric Administration produced weekly snow cover charts for the northern hemisphere land areas based on visual interpretation of visible satellite imagery. The primary data source was NOAA Polar Operational Environmental

Satellites (POES). The nadir resolution of the imagery acquired prior to 1972 was about 4 km. The Very High Resolution Radiometer (VHRR) launched in 1972 provided imagery with a spatial resolution of 1.0 km, and from November 1978 the Advanced VHRR (AVHRR) provided 1.1 km resolution data. Secondary data sources used to produce the charts included geostationary imagery, U.S. Air Force snow analyses, and surface observations (Ramsay, 1998). Geostationary data have been used from the NOAA Geostationary Operational Environmental Satellites (GOES) over North America since 1975, from the European Geostationary Meteorological Satellite (METEOSAT) over Europe since 1988, and from the Japanese Geostationary Meteorological Satellite (GMS) over Asia since 1989. Weekly charts show snow cover boundaries for the latest day of the chart week during which the surface in a region was visible in the imagery. The charts were then digitized to an 89×89 polar stereographic grid with 190 km resolution. In this process, a cell was considered to be snow-covered in a given week if it was interpreted to be at least 50% snow covered; otherwise it was considered to be snow-free. Recently, the digital NOAA dataset was re-gridded to the Northern Hemisphere 25-km EASE (Equal-Area Scalable Earth) Grid (Armstrong & Brodzik, 2002). The re-gridded data were used in this study to facilitate comparisons with other datasets.

The automated Interactive Multi-sensor snow and ice mapping System (IMS) replaced the manual snow cover analysis in April 1999. The IMS provides a daily snow and ice cover map for the NH with a resolution of 23 km (Ramsay, 1998), and a pseudo-weekly chart has been created to maintain the continuity of the previous database. It is unclear what impact this has had on the homogeneity of the data so the evaluation carried out in this study was restricted to the period when manual charting procedures were in use.

3.2. AVHRR-derived snow cover extent

Since the 1980s, several algorithms have been developed for snow monitoring from optical sensors, including the multispectral thresholds classification method (Allen et al., 1990; Gesell, 1989; Harrison & Lucas, 1989; Liu et al., 1999; Romanov et al., 2000). Other approaches for snow extent estimation include linear spectral unmixing for sub-pixel snow mapping (Appel & Salomonson, 2002; Romanov et al., 2003; Rosenthal & Dozier, 1996), and Normalized Difference Snow Index (NDSI) algorithm (Dozier, 1989; Hall et al., 1995, 2002). Considering the weekly availability and the coarse resolution of the NOAA dataset (originally 190 km) to be evaluated, the multispectral thresholds algorithm was chosen in this study to derive weekly snow cover extent from the AVHRR Polar Pathfinder twice-daily 5 km EASE-Grid composites (Fowler et al., 2002). Daily AVHRR/2 (NOAA, 2003) calibrated 5-channel data are available in the EASE-Grid composites.

The greatest difficulty in mapping snow cover from AVHRR imagery is the detection of cloud contamination. Snow and clouds both have high reflectance in the VIS and low brightness temperature in the IR bands. The high reflectance of snow drops quickly from VIS to MIR, however, while the reflectance of water clouds remains high (Dozier, 1989; Kidder & Wu, 1984). This feature has been used extensively in AVHRR snow/cloud discrimination and detection (for example, Allen et al., 1990; Gesell, 1989).

The signal received by AVHRR/2 channel 3 (3.55~3.99 μm) during the day includes two parts: reflected solar radiation and the emitted thermal radiation. In this study, the difference in brightness temperature between channel 3 and 4 (10.3~11.3 μm) was used to approximate the reflective component of channel 3 (Harrison & Lucas, 1989; Liu et al., 1999) and to separate snow from water clouds. AVHRR/2 channel 1 (0.58~0.68 μm) and channel 2 (0.725~1.05 μm) were used mainly to identify snow/clouds from other land cover types, such as bare land and water bodies. The brightness temperature of channel 4 was mainly used to discriminate between snow and ice clouds, which are usually colder than snow in the polar region (Raschke et al., 1992). A number of AVHRR/2 images were selected from which the main surface types (snow, clouds, bare land, and water bodies) can easily be determined visually. Surface snow depth and snow survey observations were used to assist in discriminating between snow and clouds. Many samples of each of the surface types were taken from the AVHRR/2 images. Thresholds for discrimination were then determined by averaging the spectral values of the surface types at each of the four AVHRR/2 channels. The thresholds were then adjusted according to snow depth and snow survey observations. A pixel was classified as snow covered if it passed all the thresholds on any day from a 7-day period in a NOAA chart week.

Calibrated AVHRR/2 data were obtained for the six selected springs from the AVHRR Polar Pathfinder twice-daily 5 km EASE-Grid composites (Fowler et al., 2002) available from the National Snow and Ice Data Center (NSIDC). Weekly snow cover extents for the period March through June were derived using the 1400 daytime data for the study area. The AVHRR-derived snow cover extent was found to be consistently less than that shown in the NOAA charts, for example, weeks 23~25 of 1997 are shown in Fig. 2.

3.3. SSM/I-derived snow cover extent

Passive microwave data have been used extensively to map snow cover parameters, for example, snow extent (Grody & Basist, 1996), snow depth (Chang et al., 1990; Kelly et al., 2003) and snow water equivalent (Goita et al., 2003; Josberger et al., 1998; Pulliainen & Hallikainen, 2001; Tait, 1998). The main advantage for high latitude snow cover monitoring is an all-weather sensing capability,

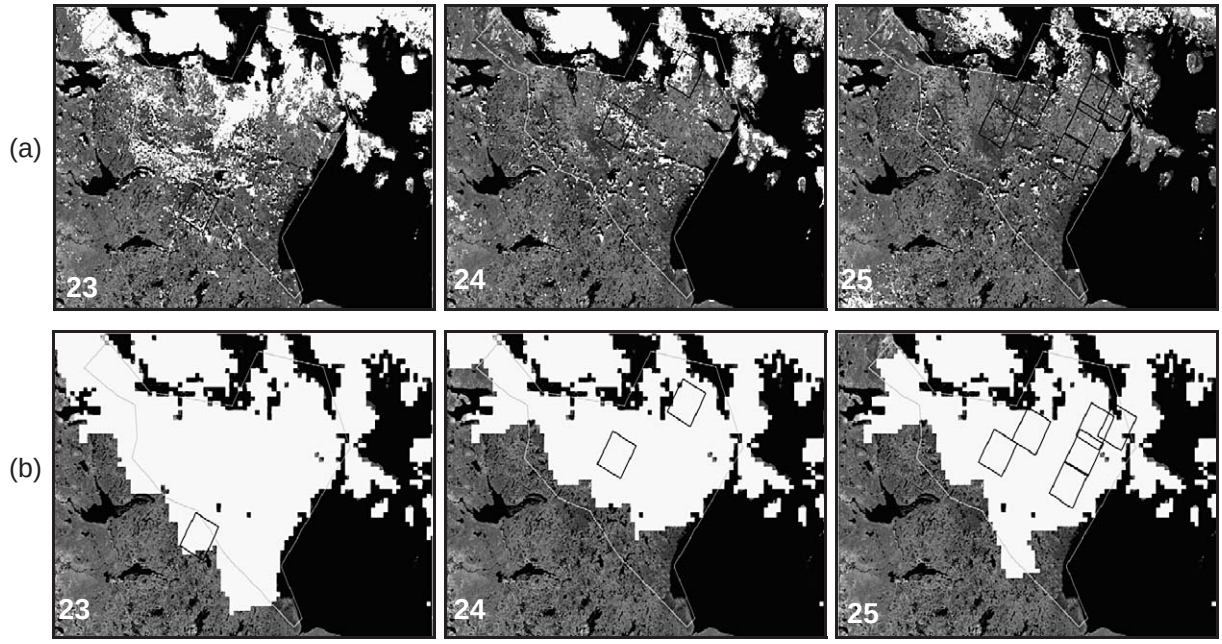

Fig. 2. Weekly snow cover maps derived from AVHRR (a) and NOAA (b) for weeks 23–25 in the spring of 1997. The nine gray boxes (one at week 23, two at week 24, and six at week 25) indicate the locations of the TM images available for each week.

while the 25 km resolution and wide swath width are well-suited for regional snow cover monitoring in non-mountainous terrain. The retrieval of snow cover information from passive microwave brightness temperatures is theoretically straightforward: as the depth and density of snow increase, so too does the amount of volume scatter of naturally emitted microwave energy. Shorter wavelength energy (i.e. 37 GHz) is more readily scattered by snow grains than longer wavelength energy (i.e. 19 GHz), so the difference in scatter between these two satellite-measured frequencies can be exploited to estimate snow water equivalent (SWE).

In reality, the relationships between snow depth, density, and microwave scatter are complicated by the physical structure of the snowpack (for example, ice lenses and snow grain size variability) and the microwave emission and scattering characteristics of overlying vegetation. There are limitations in dense forest (not an issue for our study area) and wet snow, although Walker and Goodison (1993) developed a wet snow indicator that can be used to map the spatial extent of wet snow in open prairie environments. The imaging footprint for spaceborne passive microwave data is large (resampling produces grid cell dimensions of 25 km) so these complicating factors are compounded by considerable within-grid cell variability in snowpack structure and vegetative cover.

The Climate Research Branch of the Meteorological Service of Canada (MSC) has an ongoing program to develop the retrieval of snow cover information from spaceborne passive microwave brightness temperatures for major Canadian landscape regions. This research has yielded a suite of land-cover sensitive SWE retrieval algorithms for open (Goodison & Walker, 1995) and forested (Goita et al., 2003) environments (for an overview, see Walker & Goodison, 2000). Evaluation studies have shown that SWE retrievals in open prairie environments are typically within +/− 15 mm of in situ snow surveys (Derksen et al., 2002, 2003). Systematic SWE underestimation is, however, a problem in densely forested areas because vegetation effects can mask the passive microwave signal (Derksen et al., 2003; Walker & Silis, 2002).

To date, evaluation of passive microwave SWE retrievals using the MSC open environments algorithm in tundra areas has been limited (Woo, 1998). A recently completed (March 2004) regional snow surveying campaign across approximately 500 km of northern Manitoba included a number of open tundra sites. Passive microwave derived SWE in these regions was systematically low, potentially due to the unique microwave emission and scattering characteristics of frozen lakes which comprise a high proportion of the tundra surface cover (Derksen & Walker, 2004).

In this study, SSM/I derived SWE retrievals were converted to snow extent to facilitate comparison with the NOAA snow charts, mitigating tundra SWE underestimation issues. SSM/I EASE-Grid brightness temperatures from cold overpass times (0600 hours LST) were utilized to increase the frequency of monitoring of a cold and dry snowpack-conditions which optimize algorithm performance. SCE was determined by classifying each grid cell with SWE greater than 1 mm as snow covered. The 1 mm SWE threshold for determining SCE was validated through a comparison of passive microwave derived data and NOAA snow charts in the Canadian prairies (Derksen et al., 2004) This “aggressive” threshold was used because passive

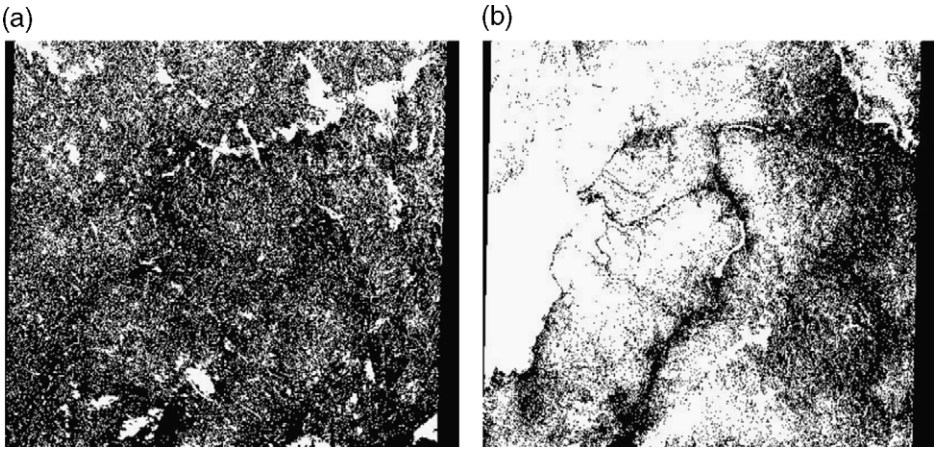

Fig. 3. Two examples of classified Landsat 5 TM browse images. Snow is shown in white. (a) June 11, 1997, 33.1% snow covered; (b) June 15, 1997, 64% snow covered.

microwave derived data tend to underestimate snow extent relative to optical data (Armstrong & Brodzik, 2001) due to problems detecting a thin and discontinuous snow cover. The absolute SWE retrievals at these low values are suspect in the context of a meaningful water equivalent, but as a proxy for snow extent, this threshold produces patterns that compare well with optically derived data (Derksen et al., 2004).

3.4. Processing of TM images

In situ snow depth observations in the study area are sparse and biased to costal regions (Fig. 1), and may not be representative of the much larger areas encompassed by pixels from the NOAA and AVHRR datasets. Therefore Landsat 5 TM browse images were used as ground truth in this study, as in Hall et al. (2002). Nine clear sky TM browse images (Fig. 2) acquired for the study area during the spring of 1997 (the year with the most clear sky TM browse images) were classified to estimate the fraction of snow-covered pixels (Fig. 3; Table 1). The resolution of the images is approximately 480 m. The TM images were classified to snow/no snow using a threshold visually determined from a trial and error separation of snow (including frozen lakes) from bare ground. The four corner coordinates (latitude/longitude) of the browse images were assessed against National Topographic Data Base (NTDB) map sheets and adjusted when necessary.

Table 1

Week	Centre lat and long	TM (%)	AVHRR-TM (%)	NOAA-TM (%)
9723 (6/2–8)	61.46° N, 103.56° W	22.7 (June 4)	−13.1	69.8
9724 (6/9–15)	65.57° N, 101.67° W	33.1 (June 11)	−11.5	66.9
9724 (6/9–15)	68.25° N, 92.60° W	64.0 (June 15)	−9.8	36.0
9725 (6/16–22)	64.20° N, 93.65° W	10.9 (June 17)	−5.7	82.1
9725 (6/16–22)	65.57° N, 92.40° W	12.6 (June 17)	−10.5	87.4
9725 (6/16–22)	66.92° N, 91.02° W	26.4 (June 17)	−21.6	75.6
9725 (6/16–22)	65.57° N, 103.21° W	14.5 (June 18)	−13.4	85.5
9725 (6/16–22)	66.92° N, 87.93° W	30.0 (June 19)	−22.5	58.9
9725 (6/16–22)	66.91° N, 98.75° W	18.5 (June 20)	−13.1	81.5
Mean			−13.5	71.5

Percent snow cover calculated from TM images (column 3) from 1997. The dates of the TM images are shown in brackets. The differences between the percent snow cover extracted from the AVHRR and NOAA datasets and those from the TM images are shown in columns 4 and 5.

4. Results

4.1. Comparison between NOAA, AVHRR, and SSM/I

The NOAA, AVHRR and SSM/I datasets were all in the EASE-Grid projection, facilitating inter-comparison. Weekly snow coverage (the fraction of snow covered pixels in the study area) was calculated from the three datasets for each of the six springs (Fig. 4). Before the onset of melt, the snow cover percentages from the three datasets are generally consistent with each other. The only exception is in week 15, 1984, when the NOAA snow cover percentage shows a sudden drop. Examining the original NOAA snow chart for that week, we found that the analyst mapped a large area as patchy snow cover. It seems that patchy snow cover was not interpreted as snow during the digitizing process. This was deduced by comparing the manual charts to the digitized datasets, as no information was found in the references. The AVHRR- and SSM/I-derived datasets produce very similar results for the timing of melt onset and the progression of melt in the study area. Compared to the AVHRR- and the SSM/I-

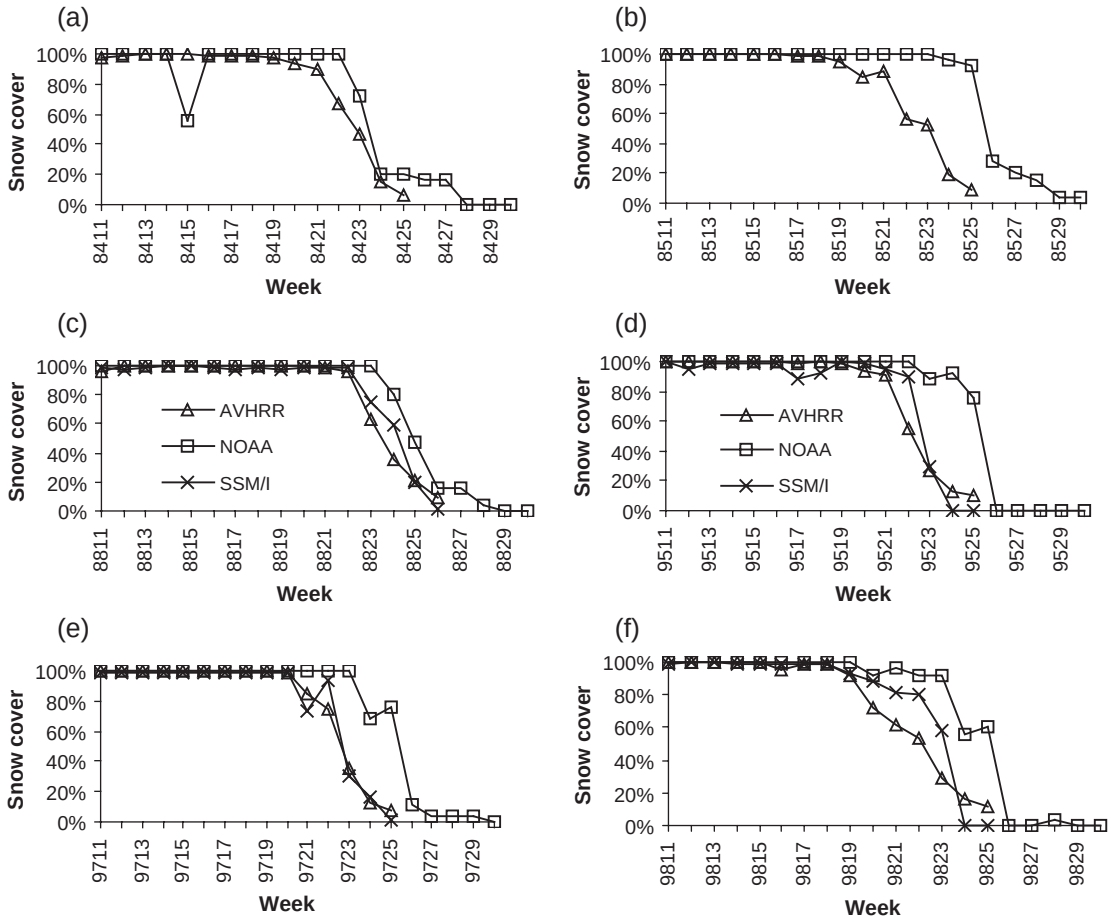

Fig. 4. Comparison of weekly snow coverage, in percent of fractional snow covered pixels in the study area from AVHRR (triangle), SSM/I (cross), and NOAA (square) for the 6 years included in the evaluation. The horizontal axis displays week (e.g. 9811 for year 1998 and week 11).

derived datasets, the onset of melt in the NOAA dataset is delayed in all 6 years. The delay ranges from about 1 week (1984 and 1988) to 2–4 weeks (other years).

4.2. Comparison between NOAA, AVHRR, and TM

We compared the snow cover fraction estimated from TM browse images (480 m) to that estimated from all the NOAA (originally 190 km) and AVHRR (5 km) pixels with center latitude/longitude falling within the TM coverage (Table 1). The area covered by the NOAA and AVHRR pixels was within 10% of the TM coverage for each of the nine browse images. Compared to the TM images, the AVHRR-derived dataset consistently underestimates snow cover. The underestimate ranges from 10.5% to 22.5%, with an average of 13.5%. This is not surprising, because the multi-spectral thresholds algorithm used in this study does not take account of mixed pixels in the AVHRR data. One threshold for a pixel to be classified as snow is that its brightness temperature is below freezing point. Bare ground is clearly present within the snow-covered area in all the TM images. Thus there are many snow-ground mixed pixels in the 5 km AVHRR data, which are not recognized as snow covered if their overall brightness temperatures are well above the freezing point. Relative to the TM dataset, the NOAA dataset consistently overestimates snow cover by 58.9–87.4%, with an average of 71.5%. This is consistent with the delay in the onset and progression of melt identified in Fig. 4.

4.3. Ground observations

Except for Lupin A and Baker Lake stations, which are located inland, all ground observation stations in the area are located along the coast. Only eight sets of in situ snow depth observations (locations are shown in Fig. 1) are available for the spring of 1997 (Meteorological Service of Canada, 2000). The daily mean air temperature for four of the eight stations was obtained from the Canadian Daily Climate Data CD-ROM (Environment Canada, 2002). Daily mean air temperature and snow depth observations for May and June 1997 are plotted in Fig. 5. The stations along the coast show very similar trends to the two inland stations. Around May 16 (in week 20), the air temperature rose above the freezing point and the snow depth decreased rapidly thereafter at most stations. The timing of these events is consistent with that of melt onset as detected by the AVHRR and SSM/I

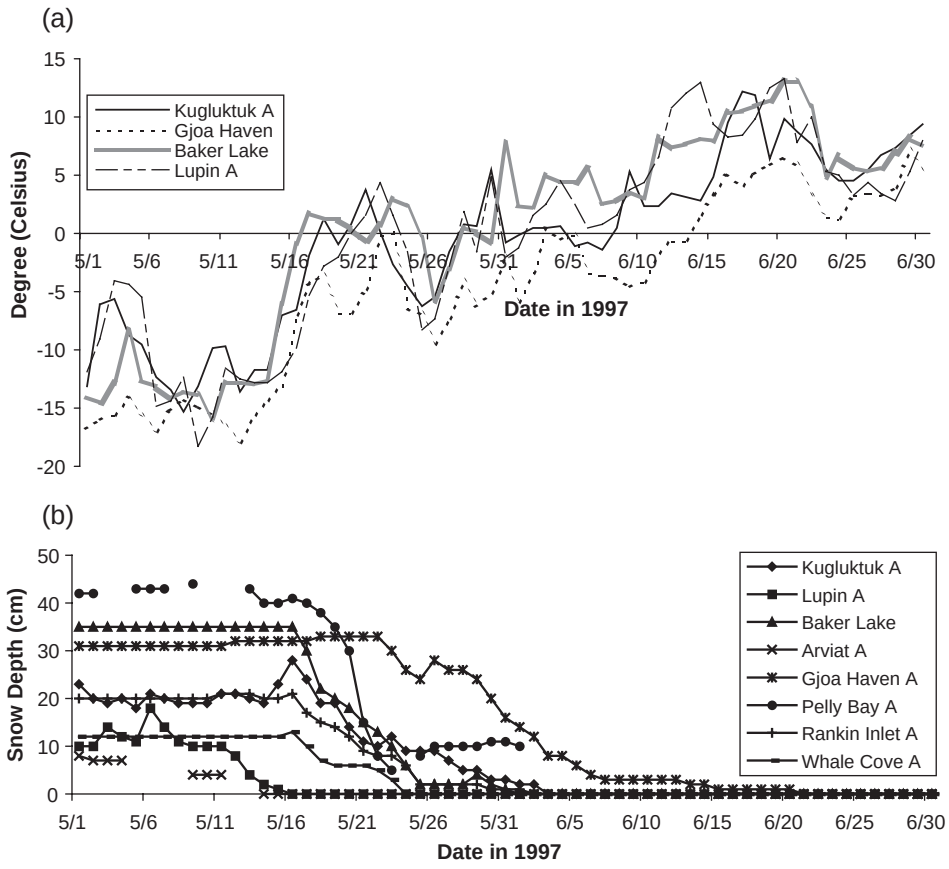

Fig. 5. Daily mean air temperature (a) and snow depth (b) in May and June of 1997.

datasets, but 3 weeks earlier than the onset of melt in the NOAA dataset (Fig. 4).

5. Discussion

Compared to the AVHRR-and SSM/I-derived snow cover extent, the NOAA dataset shows a delay in the onset of melt in all six springs. One possible explanation may lie in the different grid resolutions of the three datasets, and in the use of a 50% threshold value to differentiate between snow-covered and snow-free areas in the NOAA dataset. When considering hemispheric and continental scales, the effects of using this 50% threshold may average out and have little influence on estimates of SCE. For the smaller area investigated here, however, the 50% threshold approach would be expected to cause an apparent delay in the onset and progression of melt while snow cover is in the 100–50% range. On the other hand, the NOAA snow cover estimate would be expected to "catch-up" with the other estimates once the snow cover falls below 50%. This is not, however, observed. Experience with trying to recreate the NOAA weekly snow product from the higher resolution NOAA daily IMS product (Brasnett, pers. comm.) has revealed that a 30% snow cover fraction threshold gave the best agreement with the manual charts. This finding suggests a bias to overestimating snow cover extent in the gridded NOAA charts.

To test this hypothesis, the AVHRR-derived 5 km EASE-Grid snow dataset was remapped to the NOAA 25 km EASE-Grid using 10%, 30%, and 50% thresholds to define snow cover. As expected, the choice of a lower threshold value does reduce the difference between the NOAA and the AVHRR-derived SCE estimates (Fig. 6). Even the use of a 10% threshold, however, does not account for the whole difference. This suggests that the apparent melt delay in the NOAA dataset is not attributable solely to differences in grid resolution and the use of a 50% threshold to define snow cover.

Another possible explanation for the apparent melt delay is cloud contamination in the visible imagery used to produce the NOAA product, a problem that may be exacerbated by the reduced range of datasets available to assist in the production of the NOAA dataset at higher latitudes. For lower latitudes of North America, NOAA GOES imagery is used in addition to NOAA POES imagery to produce the snow charts. Although the NOAA GOES imagery theoretically has coverage as far as 70° N, the quality of the imagery near the margin is often not good enough to discriminate snow from clouds. The ground observing network is also concentrated below

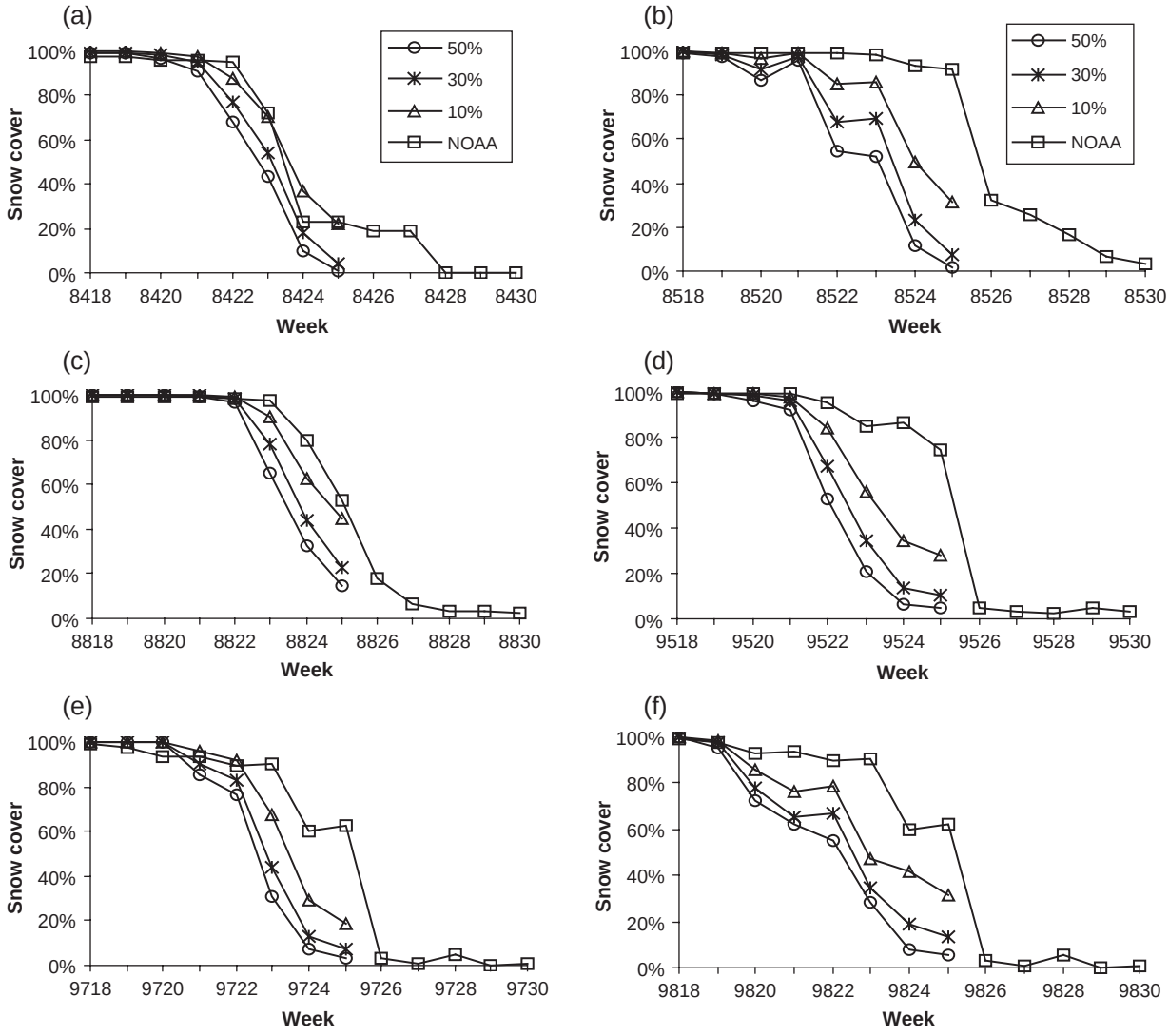

Fig. 6. Results of re-mapping 5 km AVHRR-derived snow cover to the 25 km NOAA EASE-grid applying 50%, 30%, and 10% thresholds respectively.

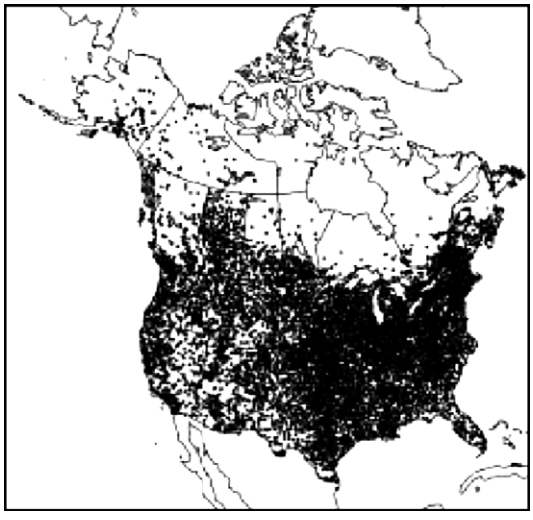

Fig. 7. Daily snow depth network over North America. Station density decreases rapidly north of about 55° N.

latitude 55° N over the more populated areas of North America (Fig. 7). Therefore, for higher latitudes, fewer in situ observations are available to verify the NOAA snow charts, which increases the chance of misclassifying clouds as snow.

Surface cloud observations for three stations in the study area are available from the Canadian Climate Normal (1971~2000) dataset (Allsopp & Morris, 2004). Monthly cloud coverage, was calculated as the percent of time in a month with cloud opacity 3–10 tenths of the sky (Fig. 8). All three stations show a similar seasonal cycle-cloud cover increases in spring, remains high in summer, and reaches its maximum in autumn. This is consistent with the surface cloud climatology for the Arctic (Curry et al., 1996). In May and June, when the NOAA dataset shows the largest difference in snow extent from the other datasets, the study area is typically more than 75% cloud covered. According to Huschke (1969), the increase of cloud amount in spring is mainly due to the increase of

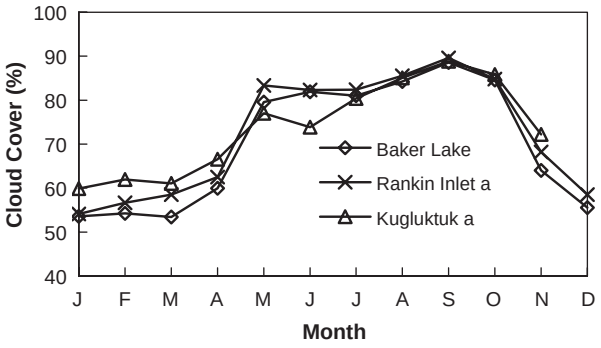

Fig. 8. Mean annual cycle of total cloud cover in percent for three stations in the study area. Data are from the Canadian Climate Normals for the 1971–2000 period.

low cloud. The annual cycle of low cloud amount ranges from ~20% in the winter to ~70% in the summer. The use of 3.7 μm data in the multi-spectral thresholds snow detection algorithm is likely to have effectively separated snow from low level liquid clouds, although the fraction of liquid cloud in the total low cloud is unknown. Such separation would be difficult to achieve using visible images alone (as would be the case for the NOAA dataset). This has also been demonstrated in several other snow/cloud discrimination studies (Key & Barry, 1989; Romanov et al., 2000).

In addition, there are many lakes in the study area. Usually water bodies remain frozen long after the snow melts on land. Robinson et al. (1993) indicated that there might be an overestimation of summer continental snow cover in the NOAA product due to difficulties in distinguishing between frozen water bodies and snow-free land in the Arctic regions. This may also contribute to the melt delay in the NOAA dataset. Available Landsat 5 TM browse images from both 1997 and 1998 were used to examine this possibility. It seems that lake ice is not the cause of the melt delay in the NOAA dataset. After week 25, many lakes were still ice-covered, but the NOAA dataset did not indicate those areas as snow covered.

The extent of the melt delay in the NOAA dataset is different for each year — about one week delay in 1984 and 1988, and 2–4 weeks delay in the other years. Studying the original manual NOAA snow charts for weeks 20–26 in all 6 years, we found large areas were depicted as patchy snow cover in charts for 1984 and 1988 in the study area. No patchy snow cover was, however, mapped in the years in which there are large differences between the NOAA dataset and the other datasets. In the case of patchy snow cover, numerical weather prediction models make larger errors if the snow cover is underestimated rather than overestimated. NOAA analysts were therefore instructed to aggressively classify snow-covered area (Peter Romanov, pers. comm.). Changes in the patchy snow cover strategy were most likely during the late 1980s and early 1990s, and there is no guarantee that the strategy was followed consistently due to the different experience levels of the analysts, and quality of the imagery used (Thomas Baldwin, pers. comm.). This indicates that the NOAA dataset may not always be consistent from year to year, which may account for the differences in melt delay in the NOAA dataset over the six springs.

If the observed spring bias applied equally across the entire period of the NOAA dataset (and this may not be the case), trends in snow disappearance date would not be affected, but it would affect trend analysis of SCE carried out on a monthly basis (e.g. trends attributed to April may actually be happening in March). The timing error would also affect correlations of monthly snow cover with other variables such as temperature (e.g. Groisman et al., 1994a, 1994b) or atmospheric circulation indices (e.g. Qian & Saunders, 2003).

6. Conclusions

Comparisons with AVHRR- and SSM/I-derived estimates of snow cover extent in the Canadian Arctic show that the NOAA weekly snow cover dataset is late in detecting the onset of melt and overestimates snow cover during the melt period in all of the six selected springs. Further investigations using Landsat TM images, near surface air temperatures, and in situ snow depth observations confirm that the NOAA dataset greatly overestimates snow cover extent in the study area during the spring melt period. Caution is therefore needed when using this dataset in any study where the timing of snowmelt is involved.

A number of factors are likely contributing to the delay in snow cover depletion in the NOAA dataset documented in this study. These include the reduced availability of satellite data at higher latitudes, frequent spring cloud cover (which is not readily differentiated from snow in visible imagery), and the limited availability of surface observations. A change in the interpretation strategy for noting patchy snow cover may account for differences between years in the magnitude of melt delay. These conclusions are also likely to apply to other regions of NH high latitudes. At lower latitudes, the NOAA GOES, European METEOSAT, and Japanese GMS imagery are available in addition to NOAA POES imagery, and there is a more extensive network of the ground observations. Further validation of the NOAA snow dataset over other high latitude regions of the NH is needed to finalize these conclusions.

Acknowledgments

This work was funded by Meteorological Service of Canada (CRYSYS program). We thank Dr. David Robinson for his review and comments, and Dr. Fiona

Cawkwell for her useful suggestions about cloud cover calculations. We are grateful to the data providers: The National Snow and Ice Data Center, Rutgers University Climate Lab Snow Data Resource Center, and the Meteorological Service of Canada.

References

Allen, R. C., Durkee, P. A., & Wash, C. H. (1990). Snow/cloud discrimination with multi-spectral satellite measurements. *Journal of Applied Meteorology*, *29*, 994–1004.

Allsopp, D., & Morris, R. (2004). Calculation of the 1971–2000 climate normals for Canada. 14th Conference on Applied Climatology, January 10–15, 2004, Seattle, WA.

Appel, I., & Salomonson, V. V. (2002). Estimate of fractional snow cover using MODIS data. *Geoscience and Remote Sensing Symposium, IGARSS'02. Int. Geosci. and Remote Sens. Soc., Toronto, Ont., Canada, 24–28 June 2002*, 3044–3046.

Armstrong, R. L., & Brodzik, M. J. (2001). Recent northern hemisphere snow extent: A comparison of data derived from visible and microwave satellite sensors. *Geophysical Research Letters*, *8*, 3673–3676.

Armstrong, R. L., & Brodzik, M. J. (2002). *Northern Hemisphere EASE-Grid Weekly Snow Cover and Sea Ice Extent Version 2*. Boulder, CO, USA: National Snow and Ice Data Center. CD-ROM.

Basist, A., Garrett, D., Ferraro, R., Grody, N., & Mitchell, K. (1996). A comparison of snow cover products derived from visible and microwave satellite observations. *Journal of Applied Meteorology*, *35*, 163–177.

Brown, R. D. (2000). Northern hemisphere snow cover variability and change, 1915–1997. *Journal of Climate*, *13*, 2339–2355.

Brown, R., & Alt, B. (2001). *The state of the Arctic cryosphere during the extreme warm summer of 1998: Documenting cryospheric variability in the Canadian Arctic*. Unpublished Report, Climate Research Branch, Downsview Ontario: Meteorological Service of Canada, 33 pp.

Chang, A., Foster, J., & Hall, D. (1990). Satellite sensor estimates of northern hemisphere snow volume. *International Journal of Remote Sensing*, *11*(1), 167–171.

Curry, J. A., Rossow, W. B., Randall, D., & Schramm, J. L. (1996). Overview of arctic cloud and radiation characteristics. *Journal of Climate*, *9*, 1731–1764.

Derksen, C., Brown, R., & Walker, A. (2004). Merging conventional (1915–1992) and passive microwave (1978–2002) estimates of snow extent and snow water equivalent over central North America. *Journal of Hydrometeorology*, *5*(5), 850–861.

Derksen, C., & Walker, A. (2004, September). Evaluating spaceborne passive microwave snow water equivalent retrievals across the Canadian northern boreal-tundra ecotone. *CD-ROM Proceedings, International Geoscience and Remote Sensing Symposium*. Alaska: Anchorage.

Derksen, C., Walker, A., & Goodison, B. (2003). A comparison of 18 winter seasons of in situ and passive microwave derived snow water equivalent estimates in western Canada. *Remote Sensing of Environment*, *88*(3), 271–282.

Derksen, C., Walker, A., LeDrew, E., & Goodison, B. (2002). Time series analysis of passive microwave derived central North American snow water equivalent imagery. *Annals of Glaciology*, *34*, 1–7.

Dewey, K. F., & Heim Jr., R. (1981). Satellite observations of variations in Northern Hemisphere seasonal snow cover. *NOAA Technidal Report NESS*, *vol. 87*. Washington, DC, 83 pp.

Dozier, J. (1989). Spectral signature of alpine snow cover from the landsat thematic mapper. *Remote Sensing of Environment*, *28*, 9–22.

Dye, D. G. (2002). Variability and trends in the annual snow-cover cycle in Northern Hemisphere land areas, 1972–2000. *Hydrological Processes*, *16*, 3065–3077.

Easterling, D. R., Karl, T. R., Gallo, K. P., & Robinson, D. A. (2000). Observed climate variability and change of relevance to the biosphere. *Journal of Geophysical Research*, *5*, 20101–20114.

Environment Canada. (2002). *CD of Canadian Daily Climate Data*. Downsview, Ontario: Meteorological Service of Canada.

Fowler, C., Maslanik, J., Haran, T., Scambos, T., Key, J., & Emery, W. (2002). *AVHRR Polar Pathfinder Twice-daily 5 km EASE-Grid Composites*. Boulder, CO: National Snow and Ice Data Center Digital media.

Frei, A., & Robinson, D. A. (1999). Northern hemisphere snow extent: Regional variability 1972–1994. *International Journal of Climatology*, *19*, 1535–1560.

Gesell, G. (1989). An algorithm for snow and ice detection using AVHRR data. An extension to the APOLLO software package. *International Journal of Remote Sensing*, *10*, 897–905.

Goita, K., Walker, A., & Goodison, B. (2003). Algorithm development for the estimation of snow water equivalent in the boreal forest using passive microwave data. *International Journal of Remote Sensing*, *24*, 1097–1102.

Goodison, B., & Walker, A. (1995). Canadian development and use of snow cover information from passive microwave satellite data. In B. Choudhury, Y. Kerr, E. Njoku, & P. Pampaloni (Eds.), *Passive Microwave Remote Sensing of Land–Atmosphere Interactions* (pp. 245–262). Utrecht, Netherlands: VSP.

Grody, N., & Basist, A. (1996). Global identification of snowcover using SSM/I measurements. *IEEE Transactions on Geoscience and Remote Sensing*, *34*(1), 237–249.

Groisman, P. Y., Karl, T. R., & Knight, R. W. (1994a). Observed impact of snow cover on the heat balance and the rise of continental spring temperatures. *Science*, *263*, 198–200.

Groisman, P. Y., Karl, T. R., Knight, R. W., & Stenchikov, G. L. (1994b). Changes of snow cover, temperature, and radiative heat balance over the northern hemisphere. *Journal of Climate*, *7*, 1633–1656.

Hall, D. K., Kelly, R. E. J., Riggs, G. A., Chang, A. T. C., & Foster, J. L. (2002). Assessment of the relative accuracy of hemispheric-scale snow-cover maps. *Annals of Glaciology*, *34*, 24–30.

Hall, D. K., Riggs, G. A., & Salomonson, V. V. (1995). Development of methods for mapping global snow cover using moderate resolution imaging spectroradiometer data. *Remote Sensing of Environment*, *54*, 127–140.

Hall, D. K., Riggs, G. A., Salomonson, V. V., DiGiromamo, N., & Bayr, K. J. (2002). MODIS snow-cover products. *Remote Sensing of Environment*, *83*, 181–194.

Harrison, A., & Lucas, R. (1989). Multi-spectral classification of snow using NOAA AVHRR imagery. *International Journal of Remote Sensing*, *10*, 907–916.

Huschke, R. E. (1969). *Arctic Cloud Statistics from "Air-Calibrated" Surface Weather Observations*. The Rand Corporation, RM-6173_PR, 79 pp.

Intergovernmental Panel on Climate Change (IPCC). (2001). Climate change. In J. T. Houghton, Y. Ding, D. J. Griggs, M. Noguer, P. J. van der Linden, X. Dai, K. Maskell, & C. A. Johnson (Eds.), *The Scientific Basis*. Cambridge University Press.

Iwasaki, T. (1991). Year-to-year variation of snow cover area in the northern hemisphere. *Journal of the Meteorological Society of Japan*, *69*, 209–217.

Josberger, E., Mognard, N., Lind, B., Matthews, R., & Carroll, T. (1998). Snowpack water-equivalent estimates from satellite and aircraft remote-sensing measurements of the Red River basin, north-central U.S.A. *Annals of Glaciology*, *26*, 119–124.

Kelly, R., Chang, A., Tsang, L., & Foster, J. (2003). A prototype AMSR-E global snow area and snow depth algorithm. *IEEE Transactions on Geoscience and Remote Sensing*, *41*(2), 230–242.

Key, J., & Barry, R. G. (1989). Cloud cover analysis with Arctic AVHRR data: 1. Cloud detection. *Journal of Geophysical Research*, *94*, 18521–18535.

Kidder, S. Q., & Wu, H. T. (1984). Dramatic contrast between low clouds and snow cover in daytime 3.7 mm imagery. *Monthly Weather Review*, *112*, 2345–2346.

Kukla, G., & Robinson, D. A. (1981). *Climatic value of operational snow and ice charts*. In Snow Watch (Ed.), 1980 (pp. 103–119). Glaciological Data, Report GD-11, World Data Center-A for Glaciology, University of Colorado, Boulder.

Liu, Y., Wang, L., & Yazaki, S. (1999). Snow cover monitoring with AVHRR data. *Recent Progress in Studies of Asian Monsoon Mechanism* (pp. 92–102). Chinese Meteorological Press.

Loveland, T., Reed, B., Brown, J., Ohlen, D., Zhu, Z., Yang, L., et al. (2000). Development of a global land cover characteristics database and IGBP DISCover from 1 km AVHRR data. *International Journal of Remote Sensing*, *21*, 1303–1330.

Meteorological Service of Canada. (2000). Canadian snow data CD-ROM. *CRYSYS Project, Climate Processes and Earth Observation Division* (pp. 92–102). Downsview, Ontario: Meteorological Service of Canada.

NOAA. (2003). http://noaasis.noaa.gov/NOAASIS/ml/avhrr.html

Pivot, F., Duguay, C., Brown, R., Duchiron, B., & Kergomard, C. (2000). Remote sensing of snow cover for climate monitoring in the Canadian subarctic: A comparison between SMMR-SSM/I and NOAA-AVHRR sensors. Proceedings of the Eastern Snow Conference, Stowe, Vermont, USA (pp. 15–25).

Pulliainen, J., & Hallikainen, M. (2001). Retrieval of regional snow water equivalent from space-borne passive microwave observations. *Remote Sensing of Environment*, *75*, 76–85.

Qian, B., & Saunders, M. A. (2003). Seasonal predictability of wintertime storminess over the North Atlantic. *Geophysical Research Letters*, *30*(13), 1698.

Ramsay, B. (1998). The interactive multisensor snow and ice mapping system. *Hydrological Processes*, *12*, 1537–1546.

Raschke, E., Bauer, P., & Lutz, H. (1992). Remote sensing of clouds and surface radiation budget over polar regions. *International Journal of Remote Sensing*, *13*, 13–22.

Robinson, D. A., Dewey, K. F., & Heim Jr., R. (1993). Global snow cover monitoring: An update. *Bulletin of American Meteorological Society*, *74*, 1689–1696.

Robinson, D. A., & Kukla, G. (1988). Comments on "comparison of northern hemisphere snow cover datasets". *Journal of Climate*, *1*, 435–440.

Romanov, P., Gutman, G., & Csiszar, I. (2000). Automated monitoring of snow cover over North America with multispectral satellite data. *Journal of Applied Meteorology*, *39*, 1866–1880.

Romanov, P., Tarpley, D., Gutman, G., & Carroll, T. (2003). Mapping and monitoring of the snow cover fraction over North America. *Journal of Geophysical Research*, *108*(D16), 8619.

Rosenthal, W., & Dozier, J. (1996). Automated mapping of montane snow cover at a subpixel resolution from the landsat thematic mapper. *Water Resources Research*, *32*, 115–130.

Saunders, M. A., Qian, B., & Lloyd-Hughes, B. (2003). Summer snow extent heralding of the winter North Atlantic oscillation. *Geophysical Research Letters*, *30*(7), 1378.

Scialdone, J., & Robock, A. (1987). Comparison of northern hemisphere snow cover datasets. *Journal of Applied Meteorology*, *26*, 53–68.

Tait, A. (1998). Estimation of snow water equivalent using passive microwave radiation data. *Remote Sensing of Environment*, *64*, 286–291.

Walker, A., & Goodison, B. (1993). Discrimination of a wet snow cover using passive microwave satellite data. *Annals of Glaciology*, *17*, 307–311.

Walker, A., & Goodison, B. (2002). Challenges in determining snow water equivalent over Canada using microwave radiometry. *Proceedings, International Geoscience and Remote Sensing Symposium, Honolulu, July, 2000* (pp. 1551–1554).

Walker, A., & Silis, A. (2002). Snow cover variations over the Mackenzie river basin from SSM/I passive microwave satellite data. *Annals of Glaciology*, *34*, 8–14.

Wiesnet, D. R., Ropelewski, C. F., Kukla, G. J., & Robinson, D. A. (1987). A discussion of the accuracy of NOAA satellite-derived global seasonal snow cover measurements. *Proceedings, Symposium on Large Scale Effects of Seasonal Snow Cover* (pp. 291–304). Vancouver, BC, Canada: IAHS.

Woo, M. -K. (1998). Arctic snow cover information for hydrological investigations at various scales. *Nordic Hydrology*, *29*, 245–266.